AAS 14-443

American Astronautical Society

American Institute of Aeronautics and Astronautics

TETHER DESIGN CONSIDERATIONS FOR LARGE THRUST DEBRIS DE-ORBIT BURNS

Lee Jasper and Hanspeter Schaub

AAS/AIAA Space Flight Mechanics Meeting

Santa Fe, NM January 26 - 30, 2014

AAS Publications Office, P.O. Box 28130, San Diego, CA 92198

AAS 14-443

TETHER DESIGN CONSIDERATIONS FOR LARGE THRUST DEBRIS DE-ORBIT BURNS

Lee Jasper[*] and Hanspeter Schaub[†]

The use of tethers in space has been considered for many years. Most recently, there have been concepts that could involve tethers for towing objects in space. Active debris removal, asteroid retrieval, and satellite servicing may require a towing vehicle with thrusting capability to maneuver the object to be towed. Because a tether does not provide a rigid interface between the two objects, post-burn collision avoidance is a critical concern. Earlier work demonstrated exciting input-shaped towing strategies that resulted in the tug and debris aligning, post-burn, with the gravity gradient stable nadir axis thus avoiding collisions. However, there is a large design space to be utilized concerning tether properties such as length, damping, and elasticity. Intermediate distances of only a few hundred meters to kilometers appear best. Elasticity is not a major factor in the system's performance. Damping however, significantly improves performance, especially for non-input shaped thrust profiles.

INTRODUCTION

Towing objects in space has been discussed frequently in recent years. Towing may be useful for active debris removal (ADR), satellite servicing, and asteroid retrieval[*]. Many of the concepts proposed to tackle these missions utilize tethers as the connection between the object of interest and the tugging body in conjunction with harpoons,[1] nets,[2] or various devices[3,4,5,6,7] such as grapples. Much effort has gone into studying the grappling devices however, the method by which the towing craft imparts energy to the object to be towed is often overlooked. Jasper et. al.[5] and Jasper and Schaub[8] have explored the tether dynamics and an open-loop input shaped control for the analysis of a tethered-tug system with the goal of avoiding collisions between the end bodies, due to the tether connection. Both of these studies are applied to the space debris and ADR problem, even though they are relevant to all towing missions.

This paper considers a maneuver that changes the orbit (eccentricity and altitude) of the tethered-tug system while achieving a stable gravity gradient nadir alignment. This paper also considers how a tether used for towing might be designed given a design space in length L_0, damping C, and elasticity E. The effect of changes to combinations of these tether properties will be analyzed based upon the desired capability to avoid collisions between the large end-bodies.

Tethers in space have been involved in a considerable number of studies.[9,10,11] They have also been demonstrated on orbit with large tether lengths. The Small Expendable Deployer System

[*]Ph.D. Candidate, Aerospace Engineering Sciences Department, University of Colorado, Boulder, CO USA.
[†]Professor, Aerospace Engineering Sciences Department, University of Colorado, Boulder, CO USA.

[*]http://www.nasa.gov/news/budget/index.html

(SEDS)[12] experiments were launched by NASA on Delta-II rockets. These tethers spanned up to 20 km kilometers. The Space Shuttle Tethered Space System (TSS) missions deployed tethers and TSS-2 reached a tether length of nearly 20 km[13†]. Several other missions have shown shorter deployments. It is therefore likely that the tether length for the tethered-tug system can span a range of distances.

Damping in tethers has received much less attention than the modeling of the undamped dynamics. However, there have been some theoretical, terrestrial and on orbit experimental analyses done concerning damping.[14,15] Characterizing the damping present in a tether, especially long tethers on orbit appears challenging. Still, damping ranges can be bounded[15] and the value of damping can also potentially be designed to reduce several of the modes of the tether.[14] A potential range of longitudinal damping coefficients is explored for the system.

Finally, Young's modulus of elasticity affects the tether's stiffness, therefore it is an important property to consider. Tethers can be made from a variety of materials but the primary material considered here is Kevlar. Kevlar does have a range of material properties, including the Young's modulus and some of that range is explored in this paper.

Figure 1 demonstrates the towing concept where a craft capable of actively thrusting (referred to as the 'tug'), is tethered to the passive object, that is, the debris to be removed or satellite to be serviced. For the satellite servicing mission, a grappling device will be utilized to attach to the asset of interest. (The method of attaching to the debris or satellite is not considered in this paper but has been studied by many other organizations.[1,2,3,4,6]) The tow vehicle can then engage its thrusters and apply the desired Δv to the asset. Note that Jasper and Schaub[8] found that the configuration can settle into a formation that oscillates about nadir, after thrusting, as shown in Figure 1. This is the desired orientation to be achieved by combining the control and a variety of tether properties.

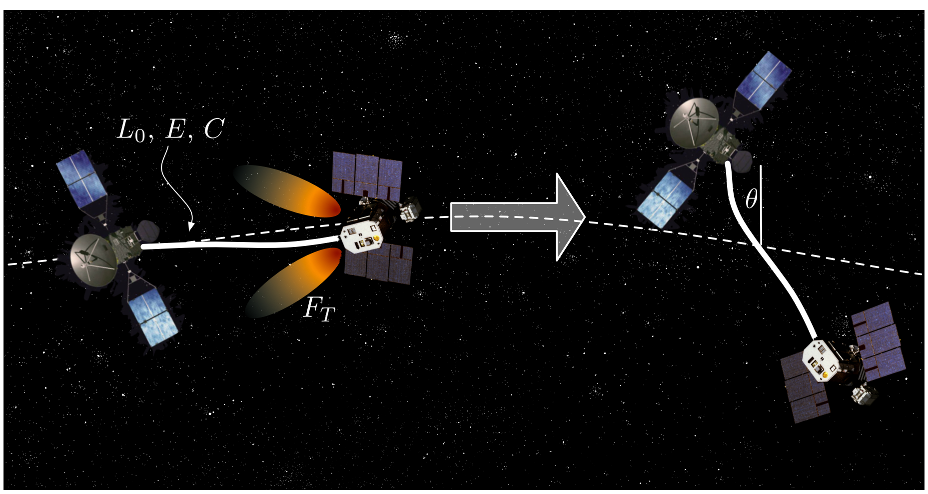

Figure 1. On orbit towing concept resulting in oscillatory motion about nadir, θ

For an ADR mission, the tug/tow vehicle is an upper stage rocket body that has delivered its primary payload to orbit. It uses its remaining fuel and payload capacity to phase to, and rendezvous with, the debris object. A secondary payload attached to the rocket then attaches a tether to the

† http://www.nasa.gov/mission_pages/shuttle/shuttlemissions/archives/sts-75.html

debris. The final fuel reserves are used to lower the periapsis of both objects, effectively removing two debris objects with a single launch. The increased drag experienced by both objects will help them to de-orbit within the 25 year rule[16,17] As an example, Reference 8 found that a vehicle in circular orbit at 800 km would deorbit in approximately 50 to 70 years. However lowering the periapsis to achieve a 425 km by 800 km orbit, the system decays in about 3 years. Depending upon initial starting altitude and amount of reserve fuel available to the active upper stage, the debris-tug system could be de-orbited within half an orbit. This concept is advantageous because it utilizes a rocket that is already going to fly and deliver a satellite to orbit. Therefore this launch is not solely for the ADR mission. Further, it is likely that the rocket's payload will require an orbit that many debris objects are already orbiting in. Figure 2 shows high-priority targets for ADR, and many of them are in heavily used orbits. These orbits are likely locations for the launch vehicle/tug to fly to. It is therefore probable that the tug will be relatively close to debris that is most important to remove from orbit.

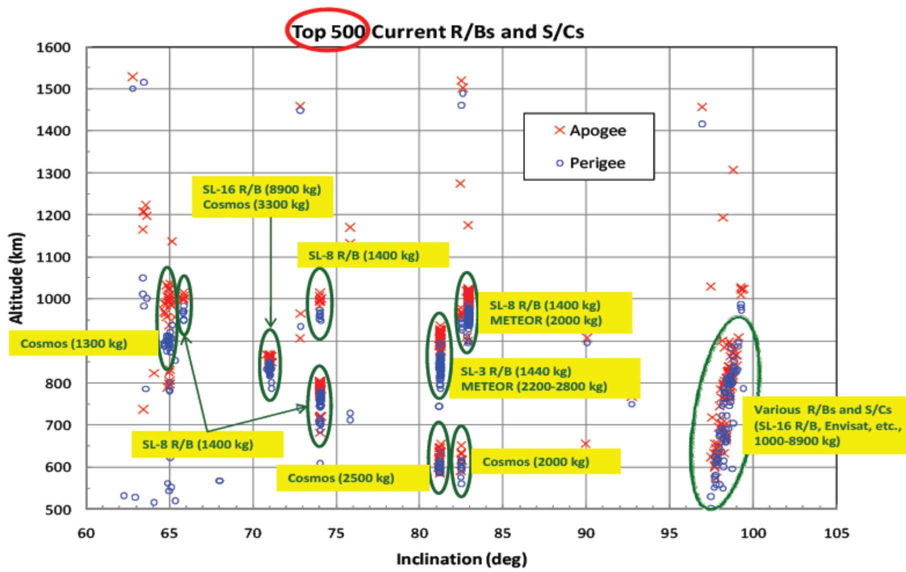

Figure 2. Current LEO environment with top 500 objects for ADR[18]

The overall aim of this research it to determine how to tow in space. Once a piece of debris is captured the fundamental questions include how should it be moved and what is the response of the system? The most important consideration is how to avoid collisions between the two end-bodies. Thrust from the tug vehicle strains the tether, giving it elastic potential energy. Once the thrust is removed from the system, the potential energy stored in the tether is released such that it pulls the two bodies together, increasing collision potential.

Using an input shaped control profile yields good results for collision avoidance.[8] This is accomplished through an open-loop control that creates a thrust profile so that the first fundamental mode of the tethered-tug system is not excited. This effectively reduces the remaining motion between the end-bodies, which gives desirable behavior in both deep-space and on-orbit simulations. A similar input shaping profile will be used in this paper.

When in orbit, the system can achieve a gravity gradient/nadir alignment, with the right conditions, as shown in Figure 1. A nadir alignment is desirable because the natural orbital dynamics will not allow the two end bodies to collide. A gravity gradient alignment is also stable and should therefore allow the two objects to remain separated indefinitely or until de-orbit occurs. This behavior is utilized for the tether properties study and is used as a metric for understanding how well the tether properties achieve this desirable configuration.

This paper utilizes the promising results given by continuous input shaping to provide a thrust and Δv to the system. However this study expands the research to consider changes to the tether properties. There are three parameters that are directly considered in this study and their affects on avoiding collisions and gravity gradient behavior are discussed. Specifically, tether length, L_0, is considered to see if there is a length that is too short or too long. The tether damping coefficient, C, and modulus of elasticity, E, are considered to see if these parameters can substitute for thrust input shaping so that a step thrust profile can be used.

First, the system model is explained along with the control input shaping method used. It should be noted that the throttle is assumed to be capable of achieving all thrust magnitudes that are commanded. Both input shaping and a step input thrust are explored. Then, each tether property is varied individually and the behavior of the system is studied. Finally, simultaneous changes to two system properties are explored.

TETHERED-TUG SYSTEM MODEL

The tethered-tug system consists of a tow vehicle that can thrust, the object to tow, and a tether between the two (Figure 1). The tug and the towed object are modeled as rigid bodies that can rotate and translate. The tether is discretized into multiple lumped point masses connected by visco-elastic forces, as shown in Figure 3. The tether starts taut in this study because slack in the tether causes

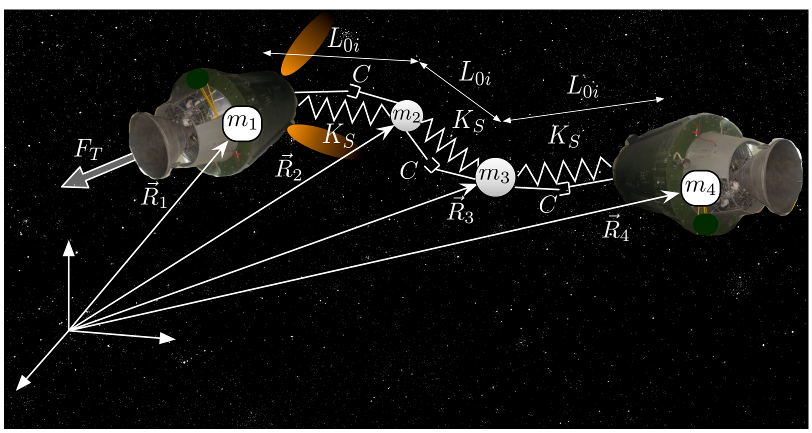

Figure 3. Discretized tether model example with 2 tether masses

amplified responses, and whipping behavior. This is not explored in this paper. The tug has active attitude control while thrusting and all the thrust is applied in the in-track/along-track direction. The attitude control is turned off when the thruster is off.

Discretized mass models for tethers are commonly used.[19,20,21,22,23] However, none of these have considered the process of towing with a tether, in space, with similar end body sizes. The translational equations of motion, caused by the tether, for the system in Figure 3 can be expressed as

$$\begin{aligned}
\ddot{\boldsymbol{R}}_i &= \tfrac{1}{m_i}\left(K_S(|\boldsymbol{R}_{i+1}-\boldsymbol{R}_i| - L_{0,i})\hat{\boldsymbol{e}}_i + C(|\dot{\boldsymbol{R}}_{i+1}-\dot{\boldsymbol{R}}_i|)\hat{\boldsymbol{e}}_i\right)\\
\ddot{\boldsymbol{R}}_{i+1} &= \tfrac{1}{m_{i+1}}\left(K_S(|\boldsymbol{R}_{i+2}-\boldsymbol{R}_{i+1}| - L_{0,i+1})\hat{\boldsymbol{e}}_{i+1} + C(|\dot{\boldsymbol{R}}_{i+2}-\dot{\boldsymbol{R}}_{i+1}|)\hat{\boldsymbol{e}}_{i+1} - m_i\ddot{\boldsymbol{R}}_i\right)\\
&\vdots\\
\ddot{\boldsymbol{R}}_N &= \tfrac{1}{m_N}\left(-K_S(|\boldsymbol{R}_N-\boldsymbol{R}_{N-1}| - L_{0,N})\hat{\boldsymbol{e}}_{N-1} - C(|\dot{\boldsymbol{R}}_N-\dot{\boldsymbol{R}}_{N-1}|)\hat{\boldsymbol{e}}_{N-1}\right)
\end{aligned} \tag{1}$$

where N is the number of masses and $\hat{e}$ defined as

$$\hat{\boldsymbol{e}}_i = \frac{\boldsymbol{R}_{i+1}-\boldsymbol{R}_i}{|\boldsymbol{R}_{i+1}-\boldsymbol{R}_i|} \tag{2}$$

These are only part of the equations of motion used for the numerical simulation used in this paper. Gravity and the thrust control acceleration are also present as well as the rigid body dynamics for the tug and debris.

The natural frequency ω_n of the system can be found by taking the complicated three-dimensional model in Figure 3 and simplifying it to a one-dimensional problem, as in Figure 4.

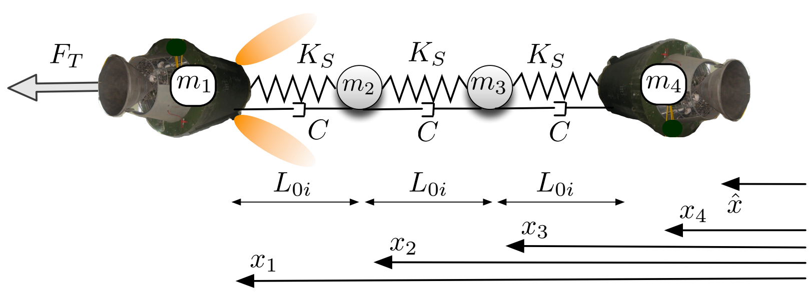

Figure 4. Discretized tether model example with 2 tether masses

The separation between the bodies can now be expressed as

$$\begin{aligned}
L_i &= |\boldsymbol{R}_{i+1}-\boldsymbol{R}_i| - L_0\\
L_i &= x_{i+1} - x_i - L_0\\
\\
\dot{L}_i &= \dot{x}_{i+1} - \dot{x}_i\\
\ddot{L}_i &= \ddot{x}_{i+1} - \ddot{x}_i
\end{aligned} \tag{3}$$

assuming all unstretched tether lengths, L_0, are the same. $\boldsymbol{R}_i$ is the position of mass i. Using the linearization in Eq. (3), the discrete mass model in a state space representation is given in Eq. (4). Here n is the number of links between each mass. Therefore, if there are four masses ($N = 4$), there are three tether links and $n = 3$.

$$\dot{\boldsymbol{X}} = [A]\boldsymbol{X} + [B]\boldsymbol{u} \tag{4}$$

The variables in Eq. 4 are given below.

$$
\boldsymbol{X}_{2n\times 1} = \begin{bmatrix} L_1 \\ \vdots \\ L_n \\ \dot{L}_1 \\ \vdots \\ \vdots \\ \dot{L}_n \end{bmatrix} \quad [B]_{2n\times 1} = \begin{bmatrix} 0 \\ \vdots \\ 0_n \\ 1 \\ 0_2 \\ \vdots \\ 0_n \end{bmatrix} \quad \boldsymbol{u} = \frac{F_T}{m_1}
$$

F_T is the thrust force, applied only to m_1. The matrix $[A]$ can be broken up into four smaller matrices:

$$
[A]_{2n\times 2n} = \begin{bmatrix} [0]_{n\times n} & [I]_{n\times n} \\ [A_{2,1}]_{n\times n} & [A_{2,2}]_{n\times n} \end{bmatrix}
$$

The acceleration caused by the visco-elastic spring force is given in Eq. 5, which is entirely position dependent.

$$
[A_{2,1}] = K_S[M] \tag{5}
$$

with

$$
[M] = \begin{bmatrix}
-\frac{(m_i+m_{i+1})}{m_i m_{i+1}} & \frac{1}{m_{i+1}} & 0_{n-1} & \cdots & 0_n \\
\frac{1}{m_{i+1}} & -\frac{(m_{i+1}+m_{i+2})}{m_{i+1}m_{i+2}} & \frac{1}{m_{i+2}} & \ddots & \vdots \\
0_{n-1} & \ddots & \ddots & \ddots & 0_{n-1} \\
\vdots & \ddots & \frac{1}{m_{n-1}} & -\frac{(m_{n-1}+m_n)}{m_{n-1}m_n} & \frac{1}{m_n} \\
0_n & \cdots & 0_{n-1} & \frac{1}{m_n} & -\frac{(m_n+m_{n+1})}{m_n m_{n+1}}
\end{bmatrix} \tag{6}
$$

m_i is each body's mass and the spring constant K_S is expressed in Eq. (7)

$$
K_S = \frac{EA}{L_0} \tag{7}
$$

with units of $\frac{N}{m}$. Here L_0 is the initial, unstretched (equidistant) length of the tether between each mass, E is the Young's modulus of elasticity for the tether, and A is the cross sectional area. Because Eq. (4) models a tether as a spring, it is only accurate while the tether is in tension. When the separation distance is less than L_0, all spring forces go to zero.

Without damping $[A_{2,2}] = [0]_{n\times n}$. Using a strain based damping model[20]

$$
\epsilon_i = \frac{|\boldsymbol{R}_{i+1} - \boldsymbol{R}_i| - L_0}{L_0} = \frac{L_i}{L_0} \tag{8}
$$

then the strain rate is

$$
\dot{\epsilon}_i = \frac{\dot{L}_i}{L_0} \tag{9}
$$

assuming L_0 is a constant. The force due to damping is then expressed as

$$
\boldsymbol{F}_{Di} = C\dot{\epsilon}_i\hat{\boldsymbol{e}}_i \tag{10}
$$

Here, C ($\frac{kg}{s}$) in Eq. (10) is the damping coefficient. With this linear damping model, $[A_{2,2}]$ becomes

$$[A_{2,2}] = C[M] \tag{11}$$

with $[M]$ from Eq. (6). This is also only correct while in tension. There is no damping present while the separation between two masses is less than L_0.

CONTINUOUS INPUT SHAPING CONTROL FORMULATION

There are two primary controls that have been considered for the tethered-tug system. The first, is a step input that thrusts in the along-track direction for the duration required to achieve a desired Δv. This is effective at changing the orbital parameters of the tug and debris but because it is a step input, all frequencies of tether are excited. This is undesirable as the collision potential between the objects is increased.

The other control method considered is open-loop input shaping on the thrust's step profile. The input shaping method used is a notch filter that attenuates the natural frequencies of the system. Reference 8 found that the first mode of the tether system is the most important to attenuate, therefore only the first mode is attenuated here. Using a doubly notched thrust profile, where the notched frequencies span a range around the fundamental mode, a robust control design is created that can withstand errors in knowledge of the mass of the towed object. This is very advantageous because the mass of a debris object or an asteroid is likely to only be an approximate value. This is referred to as the 'double notch'.

Performing an Eigen value analysis on the system, Eq. (4), the fundamental mode of the system can be found. As an example, the Eigen-frequencies ω_d of a three body (single tether mass) system are found by solving for the roots of Eq. (12).

$$z_0 + z_1\omega_d + z_2\omega_d^2 + z_3\omega_d^3 + z_4\omega_d^4 = 0 \tag{12}$$

where

$$\begin{aligned}
z_0 &= K_S^2 m_1 + K_S^2 m_2 + K_S^2 m_3 \\
z_1 &= 2CK_S m_1 + 2CK_S m_2 + 2CK_S m_3 \\
z_2 &= C^2 m_1 + C^2 m_2 + C^2 m_3 + K_S m_1 m_2 + 2K_S m_1 m_3 + k m_2 m_3 \\
z_3 &= C m_1 m_2 + 2C m_1 m_3 + C m_2 m_3 \\
z_4 &= m_1 m_2 m_3
\end{aligned}$$

The undamped natural frequencies (ω_n) can be found by setting $C = 0\ \frac{kg}{s}$. They are also given in Reference 8.

The natural frequencies of the system are given in Tables 2, 3, and 4 for each tether property study. A linear sensitivity study of the Eigen values is also performed, given each set of system properties and variability in those properties. For this paper, the sensitivity in the first natural frequency of the system, due to changes in debris mass of approximately 500 kg is considered. The Eigen values are the natural frequencies which are a function of multiple of the system properties. For example a four body system (two tether masses) produces:

$$\lambda = \omega_d = f(m_{\text{tug}}, m_2, m_3, m_{\text{debris}}, E, A, L_0, C)$$

Because of this, the sensitivity study is done by evaluating Eq. (13), which is just a first order Taylor expansion about the debris mass of the damped natural frequency obtained from the roots of Eq. (12).

$$\delta\omega_d = \left.\frac{d}{dm_{\text{debris}}}\omega_d\right|_{m_{\text{debris Expected}}} (m_{\text{debris}} - m_{\text{debris Expected}}) \tag{13}$$

Once the variability in the first natural frequency is found, the double notch transfer function can be designed so that the cutoff frequencies, ω_c, fall on either side of the natural frequency ω_d e.g. $\omega_c = \omega_d \pm \delta\omega_d$. Eq. (14) shows the double notch

$$g(s) = \frac{(s^2 + \omega_{c1}^2)(s^2 + \omega_{c2}^2)}{(s^2 + \text{BW}_1 s + \omega_{c1}^2)(s^2 + \text{BW}_2 s + \omega_{c2}^2)} \tag{14}$$

where s is the frequency, ω_{c1} is the first cut-off or notch frequency, ω_{c2} is the second cut-off or notch frequency, and $BW1$ and $BW2$ are the bandwidths for each notch. Eq. (14) can be converted into the discrete domain and the time domain in many ways. This process can be done with a Tustin (Trapezoidal) Approximation,[24] or several other methods, but is not discussed here.

The frequency domain response of the double notch can be seen in Figure 5. Reference 8 shows that an expected debris mass of 1500 kg can vary by as much as ± 500 kg and still see minimal relative motion between the two end bodies, when using a double notch.

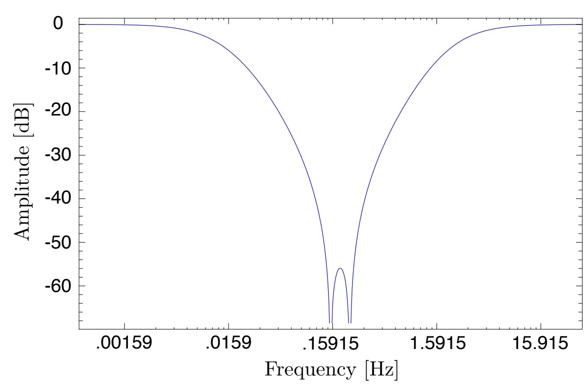

Figure 5. Double notch centered about first fundamental mode of system

TETHER PARAMETER TRADE SPACE

The basic properties for the system are given in Table 1. These values are the baseline values and are varied depending upon the simulation. As each tether property is varied, the change of the fundamental frequency for the system is given in the second column of Table 2 - 4. This frequency is the notched frequency used in the input-shaping approach. The tug and debris are based upon the Russian Soyuz upper stage and the Kosmos-3M upper stage rocket body. This has helped to define the basic mass, inertia, thrust, and Δv capabilities. The initial altitude was chosen due to its high density, and high priority, debris (Figure 2). Tether mass changes as the unstretched length changes and the volume of the tether is assumed to be a cylinder.

[‡]http://www.matweb.com/index.aspx

Table 1. Baseline vehicle, tether and simulation parameters

Tug Mass	2500 kg
Tug Inertia	diag[10208, 10208, 2813] kg m^2
Debris Mass	1500 kg
Debris Inertia	diag[1285, 6829, 6812] kg m^2
Baseline Tether Length L_0	1000 m Equal space between masses
Tether Material	Kevlar
Baseline E	170 GPa
Tether Diameter	3.2 mm
Tether Density	1470 kg/m^{3‡}
Baseline C	0 $\frac{kg}{s}$
Thrust	2009 N
Δv	100 m/s
Starting Altitude	800 km (circular)

The range of tether lengths considered was developed based upon safe distance considerations and previous flight missions.[12,13] Based upon the relative motion often seen in previous studies,[5,8] the minimum separation distance between the two end bodies should be at least 100 m. The maximum distance of 10 km is within demonstrated tether lengths from previous flight missions. The natural frequency, and its sensitivity to change in debris mass (Eq. (13)) is given in Table 2.

Table 2. Change in natural frequency, and natural frequency sensitivity with tether length, L_0**.** $E =$ 170 **GPa,** $C = 0\ \frac{kg}{s}$

L_0 (m)	ω_n (Hz)	$\pm\delta\omega_n$ (Hz)
100	0.617	0.116
500	0.273	0.051
1000	0.192	0.036
2000	0.136	0.025
5000	0.086	0.016
10000	0.061	0.011

Damping in tethers is hard to characterize and there is not much good data on the damping that occurred with tethers that have flown.[15,25] Studies that have been done show that the damping can be bounded based upon tether length and end mass size.[15] The lower bound is based upon 'structural' properties which depend upon how the tether is built. The upper bound is based upon viscous forces both internal to the tether and external (such as atmospheric drag). This gives a range on C between 1×10^-3 and about 1.10, for the tethered-tug system. However, due to the fact that the tether can be designed to achieve various material properties, a wider range will be explored. Specifically, larger values of C will be used. Longitudinal damping is considered in this paper and transverse tether damping is set to zero because it is much smaller.

Table 3. Change in natural frequency, and natural frequency sensitivity with tether damping, C. $L_0 = 1$ km, $E = 170$ GPa.

C ($\frac{kg}{s}$)	ω_d (Hz)	$\pm\delta\omega_d$ (Hz)
0.1	0.19247	0.034360
1	0.19247	0.034360
2	0.19247	0.034360
4	0.19247	0.034360
8	0.19247	0.034360
10	0.19247	0.034360

Tether stiffness directly depends upon material properties, specifically the Young's Modulus (Eq. (7)). The material frequently considered for use in space tethers is Kevlar.[9,13,15,25,26] Assuming Kevlar is the primary load bearing material, it has a fairly wide range of possible moduli to consider. This range has been explored through the use of *www.matweb.com*[§]. The natural frequency, and its sensitivity to change in debris mass (Eq. (13)) is given in Table 4.

Table 4. Change in natural frequency, and natural frequency sensitivity with Young's modulus, E. $L_0 = 1$ km, $C = 0$ $\frac{kg}{s}$

E (GPa)	ω_n (Hz)	$\pm\delta\omega_n$ (Hz)
27	0.0767	0.014
60.5	0.115	0.021
94	0.143	0.027
161	0.187	0.035
194.5	0.206	0.039
228	0.223	0.042

TETHER LENGTH

The different thrust profiles created by the double notch and changes in tether length are given in Figure 6. As the length of the tether increases the natural frequency reduces causing a slower ramp-up in thrust. These profiles are created such that they satisfy frequency notching while achieving a $\Delta v = 100$ m/s. The longer tether lengths require thrust durations that are significant relative to the orbital period (which is 6054 s at 800 km). Again, the thrust direction is aligned with the orbit frame along-track vector during the maneuver duration so that the desired orbit altitude change occurs properly.

Figure 7 and Figure 8 show the relative separation of the tether-tug system end bodies, the angle from nadir, and the tether tension for the L_0 lengths in Table 2. A nadir/gravity gradient alignment

[§]http://www.matweb.com/index.aspx

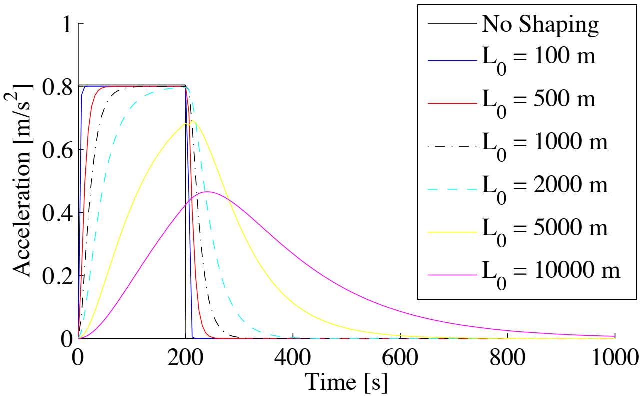

Figure 6. Thrust acceleration profiles to achieve a $\Delta v = 100$ m/s. Tether length study.

is defined as the tethered-tug system oscillating about the nadir vector (0^o) while maintaining a separation distance between the end bodies of L_0. Note that the tension in the tether is scaled in each plot so that it properly fits the 'angle from nadir' axis. Therefore, if the tension is scaled by 0.5 and its value reads 100, the actual tension is 200 N. The tension is zero at an angle of 0^o.

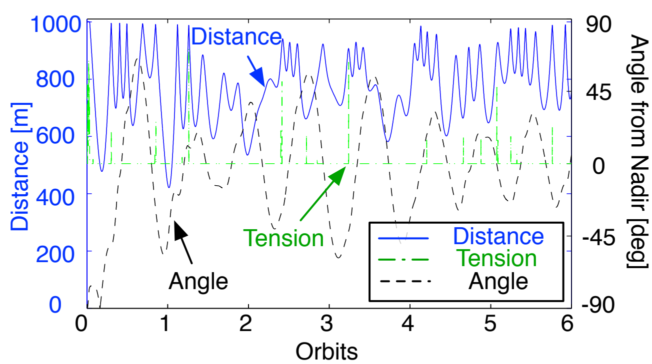

Figure 7. Relative motion and tether tension between tug and debris with a STEP input. $L_0 = 1$ km, $E = 170$ GPa and $C = 0$ $\frac{kg}{s}$. The debris' expected mass is 1500 kg but it is actually 2000 kg in simulation. Tension scaled by 0.036. Tether length study.

Figure 7 demonstrates the general motion of the tethered-tug system using a step input compared to Figure 8 that uses the notched thrust profile. While Figure 7 does see some oscillation of the formation about the nadir vector, the separation distance between the end bodies is quite dynamic and therefore this does not achieve the desirable nadir alignment. Conversely, Figure 8 shows that some of the distances do achieve desirable motion and many do maintain large separations with small tensions.

Figure 8(a) experiences a collision early on, thus, very little of the behavior is shown. Figure 8(b) demonstrates the most desirable motion with a gravity gradient oscillation occurring right after thrusting, with very little tension in the tether. It does see large oscillations about nadir, reaching about 50^o. By comparison, Figure 8(c) experiences a tumbling motion for the first four orbits, de-

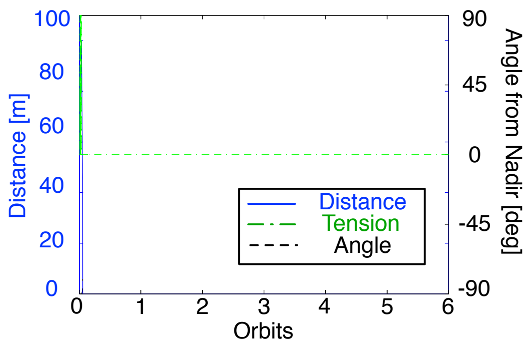

(a) $L_0 = 100$ m.

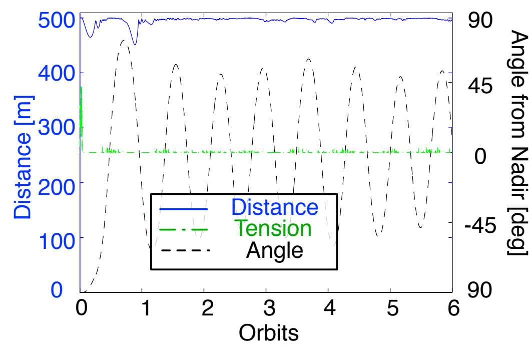

(b) $L_0 = 500$ m.

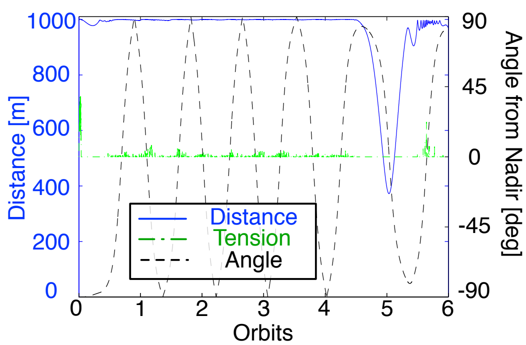

(c) $L_0 = 1000$ m.

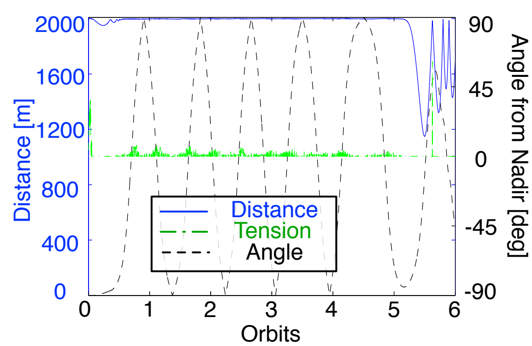

(d) $L_0 = 2000$ m.

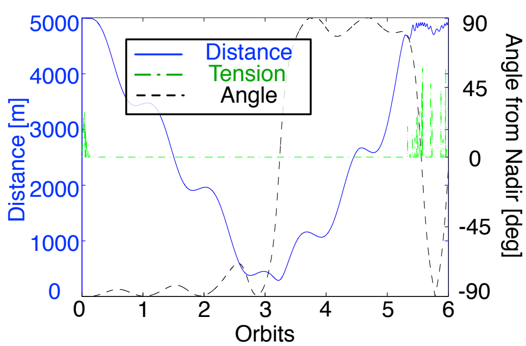

(e) $L_0 = 5000$ m.

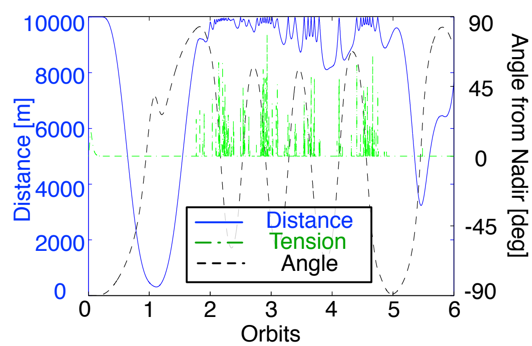

(f) $L_0 = 10000$ m.

Figure 8. Relative motion and tether tension between tug and debris with a NOTCH input. $E = 170$ GPa and $C = 0\ \frac{kg}{s}$. The debris' expected mass is 1500 kg but it is actually 2000 kg in simulation. Tension scaled by 0.036. Tether length study.

noted by the sharp points in the 'angle' line at $\pm 90^o$. However, near 4.5 orbits the formation appears to hold at near 90^o (both masses are aligned along-track), allowing the two masses to begin drifting closer together. As the two masses drift and re-tension the formation looks to settle into the desirable nadir motion. Similar behavior is seen with Figure 8(d). Based upon other simulations (Figure 10 and Figure 11) transitioning from tumbling to gravity gradient has a corresponding reduction in separation distance and the overall motion stabilizes out ofter about 1.5 orbits. Therefore, it is likely that the 1 km and 2 km distances will also settle to gravity gradient. However, Figure 8(e) and Figure 8(f) do not tumble or appear to achieve gravity gradient motion. It is interesting to note that the two furthest distances considered had the closest approaches showing that longer tethers do not guarantee further separation.

When the angle becomes large, but the system does not tumble, the separation distance reduces. This is because, at large angles, the two bodies are nearly aligned in the along-track direction. Any velocity differences will cause drift between the two bodies, thus they begin to approach each other. The end bodies generally have enough offset in the radial direction so that they pass by each other and eventually the tether catches them, causing gravity gradient motion. This behavior is consistent throughout all the results for each tether property. Generally, angles above about 70^o seem to cause this behavior.

Further, major dips in the separation distance only occur while the an end body is above, and forward of, the center of mass of the system. Being in a higher orbit than the lower body, the forward body will drift (relatively) backwards. The lower body moves faster and drifts (relatively) forwards. In all simulations, after thrusting the tug always begins with a slightly higher relative velocity that the debris (due to the thruster and being in a slightly lower orbit). The tug then increases in orbit altitude and begins swinging over the top of the formation. This causes the initial dip in relative separation distance and the transition to either tumbling or gravity gradient motion.

The overall results from the length study are given in Table 5. Again, achieving gravity gradient means that the tethered-tug system oscillates about nadir while maintaining a separation of nearly L_0. A ‘close approach’ occurs when the end bodies approach each other. Generally, using a step input, independent of tether length, causes poor performance. Several collisions occur and none of the distances considered achieve gravity gradient motion. The input shaped thrust profile performs better, with the only collision at $L_0 = 100$ m. Still, most of the lengths do not achieve gravity gradient. It also appears that as tether length gets longer, the performance reduces and more relative motion occurs.

Table 5. Summary of tether length, L_0, study. $E = 170$ **GPa,** $C = 0 \ \frac{kg}{s}$

L_0 (m)	Thrust Profile	Gravity Gradient?	Notes
100	Step	No	Collision at 2106 s
100	Notch	No	Collision at 325 s
500	Step	No	Collision at 4588 s
500	Notch	Yes	
1000	Step	No	
1000	Notch	Likely	Transition from tumble to gravity gradient around orbit 5
2000	Step	No	
2000	Notch	Likely	Motion in tether length around orbit 6
5000	Step	No	Close approach ≈31 m
5000	Notch	No	Does not tumble or nadir align
10000	Step	No	
10000	Notch	No	May achieve nadir after more time

LONGITUDINAL DAMPING

Figure 9 shows the response of the system due to a step input. It is expected that, given longitudinal damping, the tether should remain close to the full tether length and some oscillations about nadir may decay. Figure 9(b) shows that this does occur but Figure 9(a) shows that the undesirable chaotic motion can also occur with a step input. As is summarized in Table 6 only the $C = 0.1$ and $C = 2$ cases do not achieve gravity gradient. Otherwise, the damped step input performs very well. This is very different from the step responses in the L_0 and E studies which perform poorly. Damping creates very encouraging results for step input thrust profiles, which is discussed further below.

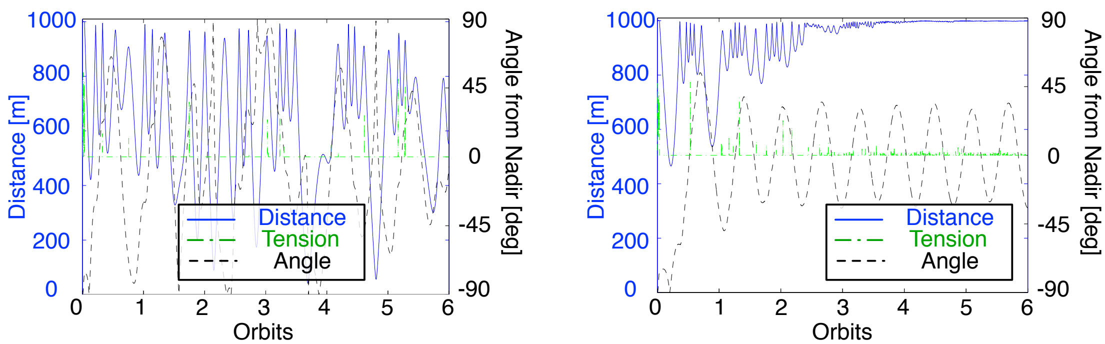

(a) $C = 0.1\frac{kg}{s}$

(b) $C = 8\frac{kg}{s}$

Figure 9. Relative motion and tether tension between tug and debris with a STEP input. $L_0 = 1$ km, $E = 170$ GPa and $C = 8\ \frac{kg}{s}$. The debris' expected mass is 1500 kg but it is actually 2000 kg in simulation. Tension scaled by 0.036. Damping study.

Figure 10 shows results from the various damping coefficients given in Table 3 while using a notch input shaped thrust profile. Figure 10 does not achieve the same amount of damping as most of the step input results. The notched results do perform well achieving a tumbling or gravity gradient motion in all cases. As expected, an input shaped thrust profile produces good results however they do not appear appreciably different than those seen for the notched results from the L_0 and E studies (Figure 8 and Figure 11).

It turns out that input shaping works against damping. Because input shaping is designed to reduce relative motion, and therefore stress in the tether, there is much less time spent in tension. This means there is less time spent damping. Depending upon the case, there is 3 to 5 times as much damping force applied during a step input compared to the notch control. This is enough to damp out the undesirable modes excited by the step input, and generally produce profiles as seen in Figure 9(b). Still, damping does occur for all of the notched profiles in Figure 9, and this helps to produce less end body relative motion, lower tensions and gravity gradient oscillations.

The two step input cases that see chaotic motion (and a collision for $C = 2$) maybe caused by several factors. First, the relative velocity between the tug and debris end bodies is slightly higher than those experienced in the other trials. The relative velocities at the end of the thrust maneuver are greater than 1 m/s for $C = 0.1$ and $C = 2$ while all other cases have a relative velocity below 1 m/s. Second, the time spent damping (time in tension) is nearly the same for these two C values,

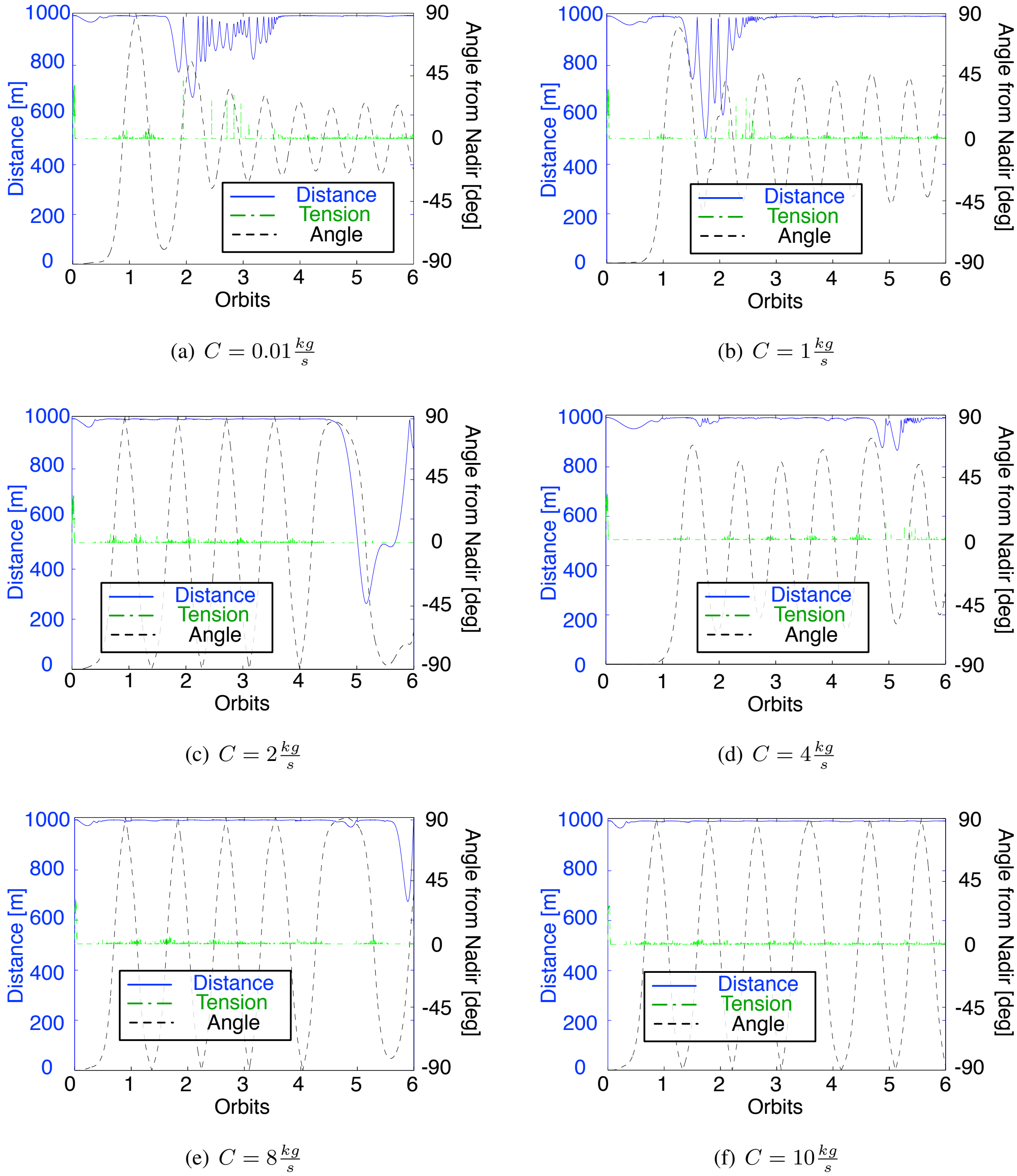

(a) $C = 0.01\frac{kg}{s}$ (b) $C = 1\frac{kg}{s}$

(c) $C = 2\frac{kg}{s}$ (d) $C = 4\frac{kg}{s}$

(e) $C = 8\frac{kg}{s}$ (f) $C = 10\frac{kg}{s}$

Figure 10. Relative motion and tether tension between tug and debris with a NOTCH input. $L_0 = 1$ km, $E = 170$ GPa. The debris' expected mass is 1500 kg but it is actually 2000 kg in simulation. Tension scaled by 0.036. Damping study.

about 280 s. The time for these two trials is less than half the next smallest value of 660 s, which occurs for $C = 1$. These differences maybe responsible for the poor performance compared to the trials for $C = 1, 4, 8, 10$.

The summary of the results from the damping study is given in Table 6. Generally, damping works best for the step input cases. All input shaped trials behave adequately and achieve gravity gradient motion.

Table 6. Summary of tether damping, C, study. $E = 170$ GPa, $L_0 = 1$ km

C ($\frac{kg}{s}$)	Thrust Profile	Gravity Gradient?	Tumble?	Notes
0.1	Step	No	No	Close approach ≈41 m
0.1	Notch	Yes	No	Tumbles 1 orbit
1	Step	Possible	No	
1	Notch	Yes	No	Tumbles 2 orbits
2	Step	No	No	Collision at 5.37 orbits
2	Notch	Possible	Tumbles	Beginning transition to grav. gradient?
4	Step	Yes	No	
4	Notch	Yes	No	No tumbling
8	Step	Yes	No	
8	Notch	Possible	Tumbles	Tumbles 4 orbits
10	Step	Yes	No	
10	Notch	No	Yes	

TETHER STIFFNESS

Figure 11 shows the relative motion, angle from nadir and tether tension of the tether-tug system for changes in E. As before with the L_0 cases, the step input produces undesirable and highly dynamic, non-nadir aligned motion similar to those seen in Figure 7. A plot is not presented for brevity. The input shaped motion in Figure 11 is much more benign and consistently achieves gravity gradient motion. Because of this the tension in the tether is often fairly low, nearly always lower than the tension created by the thrust profile, which is desirable.

There is occasionally some motion between the two end bodies over the duration considered however the motion generally does stabilize to the full length of $L_0 = 1000$ m. This is caused by either the transition from tumbling to gravity gradient (Figure 11(e) and Figure 11(e)) or large rotation angles where the two bodies are nearly aligned in the along-track direction. The general behavior is similar to that seen in the L_0 and C studies.

The results from the stiffness study are given in Table 7. Most of the step input simulations end in a collision or very close approach. This again shows that input shaping of the thrust profile is required. The notched inputs do achieve gravity gradient motion in all cases and no collisions or close approaches occur. There is some noticeable relative motion between the end bodies but this appears relatively small and does not cause the gravity gradient oscillation to stop.

STIFFNESS AND DAMPING STUDY

Due to the promising results of damping study with a step input, both Young's modulus and damping are swept to determine the behavior of the system over a wide range of values. Note, the tether length was kept constant at $L_0 = 1$ km. Table 8 summarizes the behavior of the tethered-tug system as E and C vary. The table shows whether there is a collision, tumbling motion, chaotic motion (Figure 9(a)), or gravity gradient motion. If there is a close approach, the minimum separation distance is given next to the behavior seen.

Table 7. Summary of tether stiffness, E, study. $L_0 = 1000$ m, $C = 0\ \frac{kg}{s}$

E (GPa)	Thrust Profile	Gravity Gradient?	Notes
27 27	Step Notch	No Yes	Collision Some intermediate motion
60.5 60.5	Step Notch	No Yes	Collision
94 94	Step Notch	No Yes	Collision
161 161	Step Notch	Possible Yes	Significant relative motion exists Some intermediate motion
194.5 194.5	Step Notch	No Yes	Close approach ≈6 m Some intermediate motion
228 228	Step Notch	No Yes	Collision Some intermediate motion

Table 8. Summary of tether stiffness E and damping study using a step input. $L_0 = 1$ km

$C\frac{kg}{s}$	$E = 27$ GPa	$E = 60.5$ GPa	$E = 94$ GPa	$E = 161$ GPa	$E = 194.5$ GPa	$E = 228$ GPa
0.1	Collision	Tumble	Chaotic	Chaotic (≈ 36 m)	Chaotic	Grav. Grad
1	Collision	Chaotic	Collision	Grav. Grad	Grav. Grad	Chaotic
2	Collision	Grav. Grad	Collision	Chaotic (≈ 5 m)	Collision	Grav. Grad
4	Collision	Grav. Grad	Grav. Grad	Grav. Grad	Grav. Grad	Grav. Grad
8	Grav. Grad	Grav. Grad	Grav. Grad	Grav. Grad	Grav. Grad	Grav. Grad
10	Grav. Grad	Grav. Grad	Grav. Grad	Grav. Grad	Grav. Grad	Grav. Grad

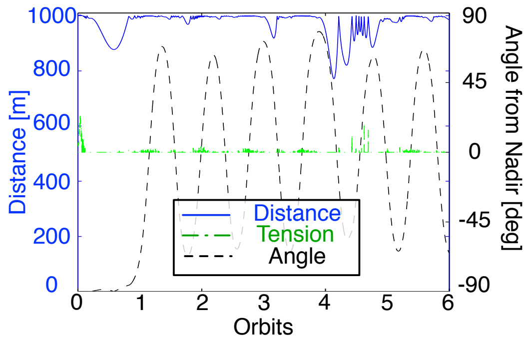

(a) $E = 27$ GPa.

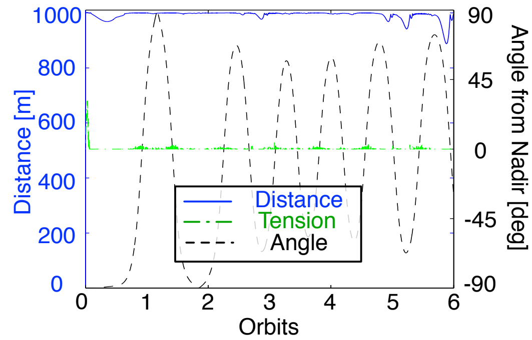

(b) $E = 60.5$ GPa.

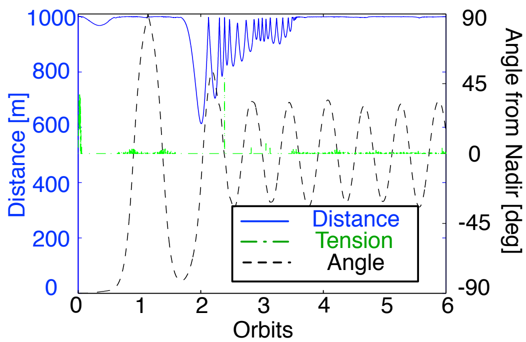

(c) $E = 94$ GPa.

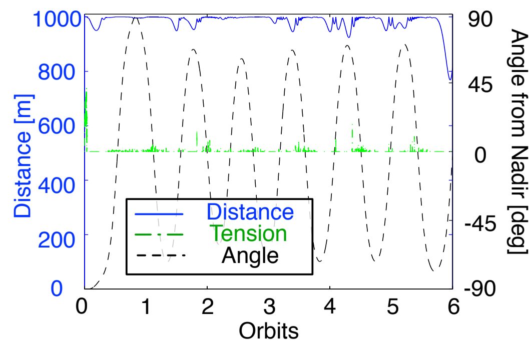

(d) $E = 161$ GPa.

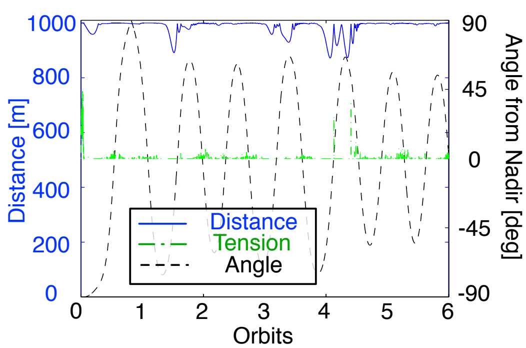

(e) $E = 194.5$ GPa.

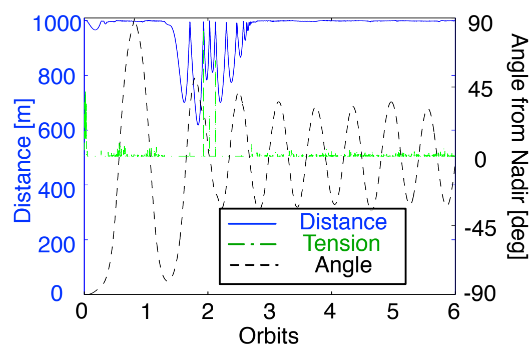

(f) $E = 228$ GPa.

Figure 11. Relative motion and tether tension between tug and debris with a NOTCH input. $L_0 = 1$ km, $C = 0\ \frac{kg}{s}$. The debris' expected mass is 1500 kg but it is actually 2000 kg in simulation. Tension scaled by 0.036. Stiffness study.

This study demonstrates some very encouraging results. First, the step input thrust profile used often causes collisions and does not achieve a tumbling or gravity gradient orientation. The results in Table 8 show that with damping, this is not true. There is a wide range of damping coefficients and elasticities that achieve desirable motion. It appears that the lower right half of the table provides good performance. One correlation that can be found is that the higher the elasticity, the less damping is needed. It also appears that with higher damping, elasticity is not a driving factor in the performance of the system. In the end, if damping is at or above $4\ \frac{kg}{s}$ and elasticity is at or above 60.5 GPa, the system achieves a taut, gravity gradient behavior.

CONCLUSION

Towing is space is a challenging prospect. There are many potential uses for such a mission but avoiding collisions between end bodies will take significant design effort. The design space for the tether is not directly intuitive and increases in length do not guarantee desirable performance. Similarly, the value of elasticity alone does not appear to significantly change system performance. However, it is very obvious that input shaping on the thrust profile is required to achieve any form of desirable performance without damping. Often the system achieves gravity gradient behavior when input shaping is used. Further, it appears that intermediate values for tether length ($L_0 = 500 - 2000$ m) achieve the best performance. Again, elasticity does not seem to drastically change performance of the system and so any stiff (Kevlar-based) tether appears acceptable.

With damping, the performance of the system significantly changes. Damping helps to moderately improve performance of an input shaped thrust profile. However, when damping is applied to the step input thrust profile, the performance is drastically improved and gravity gradient motion can be induced. It can also be concluded that higher damping with higher Young's modulus provide desirable performance for a step input. One of the most exciting results is that damping can be used as a replacement to input shaping, reducing some complexity for the rocket engine.

To implement a towing system in reality, significantly more design work is required. Still, there is a large design space for the tether many possible configuration could be utilized to realize a safe system.

ACKNOWLEDGMENTS

The authors would like to acknowledge Valery Trushkyakov, Professor in the Department of Aviation and Rocket Building, Omsk State Technical University for his contributions to the tethered rocket body ADR method.

REFERENCES

[1] J. Reed and S. Barraclough, "Development of Harpoon System for Capturing Space Debris," *Sixth European Conference on Space Debris*, Darmstadt, Germany, April 22 – 25 2013.

[2] I. Retat, B. Bischof, J. Starke, W. Froth, and K. Bennell, "Net Capture System," *2nd European Workshop on Active Debris Removal*, Quentin, Paris, France, June 18 – June 19 2012. Paper No. 4.3.

[3] D. Alary, "Astrium's views on OOS & ADR," *European On-Orbit Satellite Servicing and Active Debris Removal Conference*, Brussels, Belgium, October 30 2012.

[4] C. Bonnal and C. R. Koppel, "Getting rid of large debris: a safe low cost alternative," *2nd European Workshop on Active Debris Removal*, Quentin, Paris, France, June 18 – June 19 2012. Paper No. 3.2.

[5] L. Jasper, H. Schaub, C. Seubert, T. Valery, and E. Yutkin, "Tethered Tug for Large Low Earth Orbit Debris Removal," *AAS/AIAA Astrodynamics Specialists Conference*, Charleston, SC, Jan 31 – Feb 2 2012. Paper No. AAS 12-252.

[6] J. Reed, J. Busquets, and C. White, "Grappling System for Capturing Heavy Space Debris," *2nd European Workshop on Active Debris Removal*, Quentin, Paris, France, June 18 – June 19 2012. Paper No. 4.2.

[7] V. Trushlyakov, J. Makarov, G. Raykunov, J. Shatrov, and D. Baranovo, "The development of autonomous onboard systems for the controlled deorbiting of stages separating parts of space launch vehicle," *2nd European Workshop on Active Debris Removal*, Quentin, Paris, France, June 18 – June 19 2012. Paper No. 2.5.

[8] L. Jasper and H. Schaub, "Input Shaped Large Thrust Maneuver with a Tethered Debris Object," Vol. 96, March-April 2014, pp. 128–137.

[9] J. A. Carroll, "Tether Applications in Space Transportation," *Acta Astronautica*, Vol. 13, No. 4, 1986, pp. 165–174.

[10] M. P. Cartmell and D. J. McKenzie, "A Review of Space Tether Research," *Elsevier Progress in Aerospace Sciences*, Vol. 44, 2008, pp. 1–21.

[11] L. Johnson, B. Gilchrist, R. D. Estes, and E. Lorenzini, "Overview of Future NASA Tether Applications," *COSPAR Advanced Space Research*, Vol. 24, No. 4, 1985, pp. 1055–1063.

[12] J. A. Carroll and J. C. Oldson, "Tethers for Small Satellite Applications," *AIAA/USU Small Satellite Conference*, Logan, Utah, 1995.

[13] M. Dobrowolny and N. H. Stone, "A Technical Overview of TSS-1: the First Tethered-Satellite System Mission," *IL Nuovo Cimento*, Vol. 17, No. 1, 1994, pp. 1–12.

[14] N. N. Lee, A. H. Zorn, and M. West, "Passive Vertical Stabilization of Two Tethered Nanosatellites with Engineered Damping," *AIAA/AAS Astrodynamics Specialist Conference and Exhibit*, Honolulu, Hawaii, August 18–21 2008. Paper 2008-6450.

[15] X. He and D. Powell, "Tether Damping in Space," *Journal of Guidance Dynamics and Control*, Vol. 13, No. 1, 1990, pp. 104–112.

[16] IADC, *IADC Space Debris Mitigation Guidelines*. UNCOPUOS, Vienna, Austria, a/ac/105/c.1/l.2260 ed., 2003.

[17] K. Heiner, *Space Debris: Models and Risk Analysis*. Chichester, UK: Springer-Praxis, 1st ed., 2006.

[18] J.-C. Liou, "An active debris removal parametric study for LEO environment remediation," *Advances in Space Research*, Vol. 47, No. 11, 2011, pp. 1865 – 1876.

[19] M. Kim and C. D. Hall, "Control of a rotating variable-length tethered system," *Advances in the Astronautical Sciences*, Vol. 114, 2003, pp. 1713–1732.

[20] P. Williams, "Dynamic multibody modeling for tethered space elevators," *Acta Astronautica*, Vol. 65, 2009, pp. 399–422.

[21] F. R. Driscoll, R. G. Lueck, and M. Nahon, "Development and validation of a lumped-mass dynamics model of a deep-sea ROV system," *Applied Ocean Research*, Vol. 22, 2007, pp. 169 – 182.

[22] B. Buckham and M. Nahon, "Dynamics simulation of low tension tethers," *OCEANS'99 MTS/IEEE. Riding the Crest into the 21st Century.*, Vol. 2, 1999, pp. 757 – 766.

[23] T. P. Dreyer and D. M. Murray, "On the modeling of two-dimensional segmented representations of cable shape," *Ocean Engineering*, Vol. 11, No. 6, 1984, pp. 609 – 625.

[24] A. Tustin, "A method of analyzing the behavior of linear system in terms of time series," *JIEE, London*, Vol. 94, No. IIA, 1947, pp. 130–142.

[25] A. P. Alpatov, V. V. Beletsky, V. I. Dranovskii, V. S. Khoroshilov, A. V. Pirozhenko, H. Troger, and A. E. Zakrzhevskii, *Dynamics of Tethered Space Systems*. CRC Press, 1st ed., 2010.

[26] K. Kumar and K. D. Kumar, "Auto-Attitude Stabilization of a Twin-Satellite System Through Very Short Tethers," *Journal of Spacecraft and Rockets*, Vol. 35, No. 2, 1998, pp. 199–204.